J. Fluid Mech. (2001), *vol.* 430, *pp.* 309–333. Printed in the United Kingdom

Thin-film flow of a viscoplastic material round a large horizontal stationary or rotating cylinder

By A. B. ROSS, S. K. WILSON AND B. R. DUFFY

Department of Mathematics, University of Strathclyde, Livingstone Tower, 26 Richmond Street, Glasgow G1 1XH, UK
e-mail: s.k.wilson@strath.ac.uk; b.r.duffy@strath.ac.uk

(Received 28 October 1999 and in revised form 9 May 2000)

We consider the steady two-dimensional thin-film flow of a viscoplastic material, modelled as a biviscosity fluid with a yield stress, round the outside of a large horizontal stationary or rotating cylinder. In both cases we determine the leading-order solution both when the ratio of the viscosities in the 'yielded' and 'unyielded' regions is of order unity and when this ratio approaches zero in the appropriate distinguished limit. When the viscosity ratio is of order unity the flow consists, in general, of a region of yielded fluid adjacent to the cylinder and a region of unyielded fluid adjacent to the free surface, separated by the yield surface. In the distinguished limit the flow consists, in general, of a region of yielded fluid adjacent to the cylinder whose stress is significantly above the yield stress and a pseudo-plug region adjacent to the free surface, in which the leading-order azimuthal component of velocity varies azimuthally but not radially, separated by the pseudo-yield surface; the pseudo-plug is itself, in general, divided by the yield surface into a region of yielded fluid whose stress is only just above the yield stress and a region of unyielded fluid adjacent to the free surface whose stress is significantly below the yield stress. The solution for a stationary cylinder represents a curtain of fluid with prescribed volume flux falling onto the top of and off at the bottom of the cylinder. If the flux is sufficiently small then the flow is unyielded everywhere, but when it exceeds a critical value there is a yielded region. In the distinguished limit the yielded region always extends all the way round the cylinder, but the unyielded region does so only when the flux is sufficiently small. For a rotating cylinder a film with finite thickness everywhere is possible only when the flux is sufficiently small. Depending on the value of the flux and the speed of rotation the flow may be unyielded everywhere, have a yielded region on the right of the cylinder only, or have yielded regions on both the right and left of the cylinder. At the critical maximum flux the maximum supportable weight of fluid on the cylinder is attained and the pseudo-yield, yield and free surfaces all have a corner. In the distinguished limit there are rigid plugs (absent in the stationary case) near the top and bottom of the cylinder.

1. Introduction

A great number of materials, ranging from many of the paints and inks used in industrial coating applications to numerous muds and lavas found in geophysical contexts, are 'viscoplastic', that is to say they behave essentially like rigid solids when subjected to a small stress but flow readily ('yield') when subjected to a large

stress. Various constitutive equations have been proposed to model these viscoplastic materials; for an overview of such models and the types of flow problems that have been considered see the comprehensive review articles by Bird, Dai & Yarusso (1983) and Barnes (1999).

Much of the literature involving flow of viscoplastics has concentrated on the idealized case of a 'Bingham' material, that is, a material that behaves like a perfectly rigid solid 'plug' unless the stress exceeds the yield stress, but otherwise behaves like a viscous fluid. For example, Bird *et al.* (1983) considered rectilinear flow of a Bingham material with rigid plugs in various geometries, Lipscomb & Denn (1984) and Tichy (1991) considered thin-film flow in various confined geometries, while Liu & Mei (1989, 1994), Huang & García (1997) and Balmforth & Craster (1999) investigated thin-film flow down an inclined plane. A generalization of the Bingham model is the Herschel–Bulkley model, and thin-film flow of a Herschel–Bulkley material down an inclined plane has been investigated by Coussot (1994), Coussot & Proust (1996), Di Federico (1998), Huang & García (1998) and Balmforth & Craster (1999).

Recent advances in experimental techniques (see, for example, Barnes 1999) have revealed that the concept of a well-defined yield stress below which no flow occurs enshrined in the Bingham model is rather idealized, and that typically materials flow very slowly even at very low stresses, that is, there is in reality no well-defined yield stress. Nevertheless, the Bingham model has proved to be a very useful one in a wide range of practical applications. However, even in steady two-dimensional flow, the use of the Bingham model for thin-film flows is not without its complications. As many authors have pointed out, a naive treatment of non-rectilinear flows gives rise to the so-called 'Bingham paradox', namely that regions of material that appear to have a stress below the yield stress (and which are therefore supposed to behave like a rigid plug) are found to be deforming. Evidently, as Lipscomb & Denn (1984) pointed out, perfectly rigid plugs are possible only in strictly rectilinear flow. An additional complication of using the Bingham model is that by assuming that any unyielded regions are perfectly rigid we, in general, deprive ourselves of any means of determining the stresses within them (Walton & Bittleston 1991; Wilson 1999).

In an important recent paper Balmforth & Craster (1999) demonstrated that the earlier work by Walton & Bittleston (1991) on rectilinear axial flow of a Bingham material through a narrow eccentric annulus contained the essence of the resolution of the Bingham paradox. Balmforth & Craster (1999) showed that, when interpreted correctly, the Bingham model does in fact lead to a consistent description of non-rectilinear thin-film flow. In particular, Balmforth & Craster's (1999) careful asymptotic analysis of non-rectilinear thin-film flow of a Bingham material down an inclined plane in the limit $\epsilon \to 0$, where ϵ (defined in § 3) is the aspect ratio of the film, reveals that the solution consists of two regions, namely a region of yielded fluid adjacent to the substrate (called the 'fully plastic' region by Balmforth & Craster 1999) in which the stress is significantly (specifically $O(1)$) above the yield stress, and a 'pseudo-plug' region of yielded fluid adjacent to the free surface in which the leading-order longitudinal component of velocity varies longitudinally but not transversely and in which the stress is only just (specifically $O(\epsilon)$) above the yield stress; these two regions are separated by a 'pseudo-yield' surface (called the 'fake yield surface' by Balmforth & Craster 1999). Since in the non-rectilinear flow considered by Balmforth & Craster (1999) the stress in the fluid is everywhere above the yield stress the entire flow is yielded and hence the apparent paradox disappears. Moreover, this analysis also reveals that the pseudo-yield surface is precisely the same as the 'yield surface' calculated from the naive approach, and so the apparently

paradoxical solutions obtained by earlier authors can in fact be justified by identifying the 'unyielded regions' as pseudo-plug regions and the 'yield surfaces' as pseudo-yield surfaces. Similar pseudo-plug regions were also obtained by O'Donovan & Tanner (1984) in their numerical investigation of axisymmetric squeeze flow, as well as by Walton & Bittleston (1991) and Beverly & Tanner (1992) in their analytical and numerical studies of rectilinear axial flow in a narrow eccentric annulus.

Wilson (1999) independently performed a more general version of Balmforth & Craster's (1999) calculation using the more realistic biviscosity model (which permits flow below the 'yield stress' and in which the stresses within any unyielded regions are determined) instead of the idealized Bingham model. Wilson's (1999) study of pressure-driven flow in a non-parallel-sided symmetric channel resolves the difficulties in the earlier (incomplete) analyses by Liu & Mei (1990), Wilson (1993) and Burgess & Wilson (1996) of, respectively, flow down an inclined plane, axisymmetric squeeze-film flow between parallel discs and axisymmetric spin coating. Specifically, Wilson (1999) adopted a biviscosity model with a yield stress from which the familiar Newtonian model is recovered in the case $\lambda = 1$ and the Bingham model is recovered in the limit $\lambda \to 0$, where λ (defined in § 2) is a ratio of viscosities in the 'yielded' and 'unyielded' regions, which are separated by the 'yield surface' on which the stress is equal to the yield stress. In particular, Wilson (1999) investigated the distinguished limit $\lambda \to 0$ (the Bingham limit) and $\epsilon \to 0$ (the thin-film limit) in which $k = \epsilon/\lambda = O(1)$. In this limit the solution again has, in general, a yielded region adjacent to the substrate in which the stress is significantly (specifically $O(1)$) above the yield stress, separated by a pseudo-yield surface from a pseudo-plug region adjacent to the free surface in which the leading-order longitudinal component of velocity varies longitudinally but not transversely. However, unlike in the case of a Bingham material, the pseudo-plug is now, in general, divided into a yielded region adjacent to the pseudo-yield surface in which the stress is just (specifically $O(\epsilon)$) above the yield stress, and an unyielded region adjacent to the free surface in which the stress is significantly (specifically $O(1)$) below the yield stress, these two regions being separated by the yield surface. The location of the yield surface (but not that of the pseudo-yield surface) depends on k. In the limit $k \to 0$ (corresponding to taking the thin-film limit $\epsilon \to 0$ and then the Bingham limit $\lambda \to 0$) the yield surface coincides with the pseudo-yield surface and so the yielded part of the pseudo-plug is absent, while in the limit $k \to \infty$ (corresponding to taking the Bingham limit $\lambda \to 0$ and then the thin-film limit $\epsilon \to 0$) the unyielded part of the pseudo-plug is absent and the results of Balmforth & Craster (1999) are recovered. It is, however, important to realize that Balmforth & Craster's (1999) work shows that it is not necessary to 'relax' the Bingham model in this or any other way in order to resolve the Bingham paradox.

We remark that Balmforth & Craster's (1999) and Wilson's (1999) analyses also provide the correct solution to the problem of thin-film flow of a Bingham material in a symmetric contraction treated by Gans (1999). Ross (2000) gives details of this.

In this paper we consider the steady two-dimensional thin-film flow of a viscoplastic material, modelled as a biviscosity fluid with a yield stress (described in § 2), round a large horizontal stationary or rotating cylinder. The corresponding Newtonian problems were investigated by Nusselt (1916*a*, *b*), Moffatt (1977) and Duffy & Wilson (1999). The biviscosity model used by Wilson (1999) is preferred to the idealized Bingham model used by Balmforth & Craster (1999) first because it is a more realistic model for real viscoplastic materials and secondly because it allows the stresses within any unyielded regions to be determined without making any additional assumptions. In § 3 we obtain the leading-order solutions in the case $\lambda = O(1)$ as $\epsilon \to 0$ and in

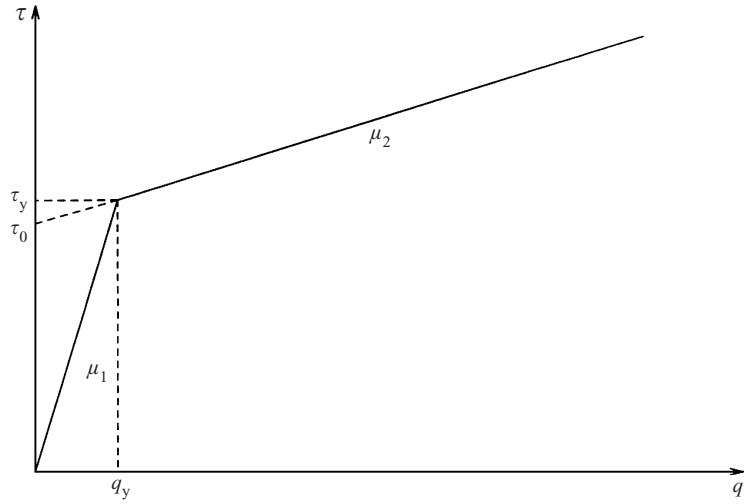

FIGURE 1. The biviscosity model.

the distinguished limit $\lambda \to 0$ and $\epsilon \to 0$ in which $k = \epsilon/\lambda = O(1)$. We then employ these solutions to describe flow round a stationary cylinder in § 4 and § 5, and round a rotating cylinder in § 6 and § 7. We summarize our results in § 8.

2. A biviscosity fluid

The governing equations representing conservation of mass and balance of momentum for steady slow flow of an incompressible fluid with constant density ρ take the form

$$\nabla \cdot \boldsymbol{u} = 0, \quad \nabla \cdot \boldsymbol{\sigma} + \rho \boldsymbol{g} = \boldsymbol{0}, \tag{1}$$

where $\boldsymbol{u}$, $\boldsymbol{\sigma}$ and $\boldsymbol{g}$ denote the fluid velocity, stress tensor and acceleration due to gravity, respectively. In the present work we shall consider a biviscosity fluid with a yield stress whose constitutive law is given by

$$\boldsymbol{\sigma} = -p\boldsymbol{I} + \boldsymbol{\sigma}', \quad \text{where } \boldsymbol{\sigma}' = \begin{cases} 2\mu_1 \boldsymbol{e}, & \tau \leqslant \tau_y, \\ 2\left(\mu_2 + \dfrac{\tau_0}{q}\right)\boldsymbol{e}, & \tau > \tau_y, \end{cases} \tag{2}$$

in which p is the pressure, $\boldsymbol{I}$ is the identity tensor, $\boldsymbol{e}$ is the rate-of-deformation tensor, q is the local shear rate and τ is a scalar measure of the local stress, given by

$$\boldsymbol{e} = \tfrac{1}{2}[(\nabla \boldsymbol{u}) + (\nabla \boldsymbol{u})^T], \quad q = [2\,\mathrm{tr}(\boldsymbol{e}^2)]^{1/2}, \quad \tau = [\tfrac{1}{2}\,\mathrm{tr}(\boldsymbol{\sigma}'^2)]^{1/2}. \tag{3}$$

The other five quantities in (2), namely μ_1, μ_2, τ_0, τ_y and q_y, are constant material parameters related by $\tau_y = \mu_1 q_y = \mu_2 q_y + \tau_0$ (so that only three of the five are independent). The parameters μ_1 and μ_2 are viscosities, and τ_0 and τ_y are measures of stress; τ_y is the yield stress, corresponding to the shear rate q_y. The relation between τ and q is given by $\tau = \mu_1 q$ when $q \leqslant q_y$ and $\tau = \mu_2 q + \tau_0$ when $q > q_y$, and is shown in figure 1. We note that $\tau_0 = \tau_y(1 - \lambda)$, where the viscosity ratio λ is defined by $\lambda = \mu_2/\mu_1$. For $\tau \leqslant \tau_y$ the fluid is 'unyielded' and behaves like a Newtonian fluid with a 'high' (constant) viscosity μ_1, while for $\tau > \tau_y$ the fluid is 'yielded' and behaves like a viscous fluid with a 'low' (shear-rate-dependent) viscosity $\mu_2 + \tau_0/q$. In the present

viscoplastic context $\mu_2 \leqslant \mu_1$ and so $0 < \lambda \leqslant 1$. Any surface on which $\tau = \tau_y$ which separates yielded and unyielded regions is called a 'yield surface'. The familiar case of a Newtonian fluid with constant viscosity is recovered in the case $\lambda = 1$ and the Bingham model is recovered in the limit $\lambda \to 0$.

3. Problem formulation

Consider the steady two-dimensional flow of the viscoplastic material described in § 2 round the outside of a large horizontal cylinder of radius R. We shall consider both the case when the cylinder is stationary and the case when it is rotating in a counter-clockwise sense about its horizontal axis with constant angular speed Ω (so that the circumferential speed is $U = R\Omega$). Hereafter all quantities will be made dimensionless using the radial length scale $h_y = \tau_y/\rho g$, the azimuthal length scale R, the azimuthal velocity scale $\rho g h_y^2/\mu_2$ and the stress scale τ_y. Provided that the fluid film is sufficiently slender, that is, provided that the aspect ratio of the film $\epsilon = h_y/R$ is sufficiently small, the leading-order approximation to the local behaviour is simply that of rectilinear flow with volume flux Q on a locally planar substrate inclined at an angle $\alpha = \pi/2 - \theta$ to the horizontal and moving parallel to itself with constant speed U, where θ is the conventional polar angle measured anti-clockwise from the horizontal, as shown in figure 2. Referred to the local Cartesian coordinate system $Oxyz$ shown in figure 2, the substrate has velocity $U \geqslant 0$ in the direction Ox and the local components of the fluid velocity in the directions Ox and Oz are denoted by u and w respectively.

3.1. *The solution in the case* $\lambda = O(1)$

When the viscosity ratio λ is of order unity as the aspect ratio ϵ approaches zero equations (2) and (3) give $\tau = |\sigma_{xz}|$ and $q = |\mathrm{d}u/\mathrm{d}z|$ at leading order. In general, the solution in this case comprises a region $0 \leqslant z < H$ of yielded fluid (region 2) and a region $H \leqslant z \leqslant h$ of unyielded fluid (region 1), where the leading-order locations of the yield surface and the free surface are denoted by $z = H(\theta)$ and $z = h(\theta)$, respectively. The geometry of the local problem in this case is shown in figure 2(*a*). We define the term 'yielded zone' to correspond to those values of θ at which region 2 is present; at other values of θ (the 'unyielded zone') region 2 is absent and the fluid is unyielded across the entire thickness of the film.

At leading order in the yielded zone the governing equations (1) with the constitutive equation (2) reduce to simply

$$u_{1,x} + w_{1,z} = 0, \quad \lambda^{-1} u_{1,zz} = \cos\theta, \quad p_{1,z} = -\sin\theta \tag{4}$$

in region 1 and to

$$u_{2,x} + w_{2,z} = 0, \quad u_{2,zz} = \cos\theta, \quad p_{2,z} = -\sin\theta \tag{5}$$

in region 2. Equations (4) and (5) are subject to the boundary conditions $p_1 = 0$ and $u_{1,z} = 0$ on $z = h$, $u_2 = U$ on $z = 0$, and $u_1 = u_2$, $p_1 = p_2$ and $\lambda^{-1} u_{1,z} = u_{2,z} - (1-\lambda)S$ on $z = H$, where $S = -\mathrm{sgn}(u_{2,z})$; these represent continuity of normal stress and tangential stress on the free surface, no slip on the cylinder, and continuity of velocity, normal stress and tangential stress at the yield surface respectively. The yield condition, $\tau = 1$ on $z = H$, gives $|u_{1,z}| = |u_{2,z}| = \lambda$ on $z = H$. Thus we obtain the hydrostatic pressure distribution $p = (h - z)\sin\theta$ throughout the fluid, and the velocity distributions

$$u_1 = U - \tfrac{1}{2}\lambda\cos\theta(2h - z)z - \tfrac{1}{2}(1-\lambda)[(2h - H)\cos\theta - 2S]H, \quad H \leqslant z \leqslant h, \tag{6}$$

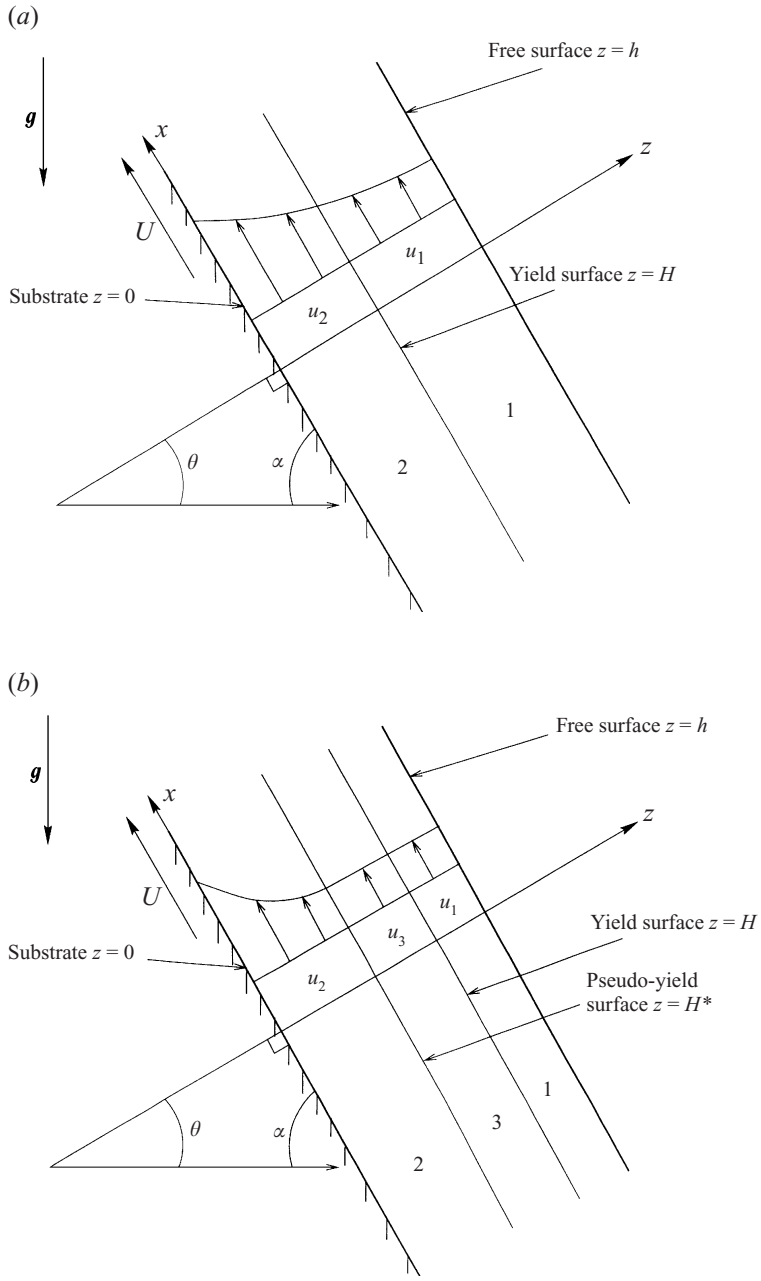

FIGURE 2. Locally rectilinear flow on a locally planar substrate inclined at an angle $\alpha = \pi/2 - \theta$ to the horizontal moving parallel to itself with speed U when (*a*) $\lambda = O(1)$, and (*b*) in the distinguished limit $\lambda \to 0$ and $\epsilon \to 0$ with $k = \epsilon/\lambda = O(1)$.

$$u_2 = U - \tfrac{1}{2}\cos\theta(2h - z)z + S(1 - \lambda)z, \quad 0 \leqslant z < H, \tag{7}$$

in regions 1 and 2 respectively. The volume flux of fluid, Q, is therefore

$$Q = Uh - \tfrac{1}{3}\cos\theta[\lambda(h - H)^3 + h^3 - (h - H)^3] - \tfrac{1}{2}S(1 - \lambda)(H - 2h)H, \tag{8}$$

and the yield condition gives

$$1 = (h - H)|\cos\theta|. \tag{9}$$

From (2) the stress throughout the fluid is given by $\tau = |\sigma_{xz}| = (h - z)|\cos\theta|$, from which it can be shown that $S = -\mathrm{sgn}(u_{1,z}) = \mathrm{sgn}(\cos\theta)$, so that the velocity gradient across the entire thickness of the film takes the opposite sign from $\cos\theta$.

At leading order in the unyielded zone we recover the appropriately non-dimensionalized version of the familiar solution for a Newtonian fluid with viscosity μ_1, namely

$$u = U - \tfrac{1}{2}\lambda\cos\theta(2h - z)z, \quad Q = Uh - \tfrac{1}{3}\lambda\cos\theta\, h^3, \tag{10}$$

as given, for example, by Moffatt (1977).

Note that H and h depend on θ only through $\cos\theta$ and hence have top-to-bottom symmetry.

3.2. *The solution in the distinguished limit $k = \epsilon/\lambda = O(1)$*

In the distinguished asymptotic limit in which both the viscosity ratio λ and the aspect ratio ϵ approach zero with $k = \epsilon/\lambda = O(1)$ the situation is somewhat more complicated. As Wilson (1999) describes, in general the solution in this limit has three regions rather than the two regions present in the case $\lambda = O(1)$. In $0 \leqslant z < H^*$ (region 2) the fluid is yielded with $u_z = O(1)$, in $H^* \leqslant z < H$ (region 3) the fluid is yielded with $u_z = O(\epsilon)$ and in $H \leqslant z \leqslant h$ (region 1) the fluid is unyielded with $u_z = O(\epsilon)$, where $z = H(\theta)$ and $z = h(\theta)$ are the yield surface and free surface encountered previously, and $z = H^*(\theta)$ is the 'pseudo-yield surface' at which u_z changes from $O(\epsilon)$ to $O(1)$. The stress is $O(1)$ below the yield stress in region 1 and $O(1)$ above the yield stress in region 2, but only $O(\epsilon)$ above the yield stress in region 3. The geometry of the local problem in this case is shown in figure 2(*b*). We will refer to regions 1 and 3, in which the leading-order solution for u varies with θ but not z, as a 'pseudo-plug' in order to distinguish them from a rigid plug in which the velocity is constant. The definitions of the yielded and unyielded zones are as before; however, in this case the yielded zone will comprise, in general, both 'partially yielded zones' (in which regions 1, 2 and 3 are present) and 'fully yielded zones' (in which only regions 2 and 3 are present). The details of the solution are given by Ross (2000), who shows that in the yielded zone H^*, H and h satisfy

$$Q = Uh - \tfrac{1}{6}\cos\theta(3h - H^*)H^{*2}, \tag{11}$$

$$(h - H^*)|\cos\theta| = 1, \tag{12}$$

$$(h - H)^2\cos^2\theta + k^2\left[\frac{\mathrm{d}}{\mathrm{d}\theta}\{H^{*2}\cos\theta\}\right]^2 = 1. \tag{13}$$

Equations (11), (12) and (13) are the volume flux, pseudo-yield and yield conditions, respectively, and are equivalent to the corresponding equations derived by Wilson (1999) (namely, his equation (9), his condition $Gy_c = 1$ and his equation (7), respectively) for pressure-driven thin-film flow of a biviscosity fluid in a non-parallel-sided symmetric channel. Using (12) to eliminate h from (11) yields

$$\tfrac{1}{3}H^{*3}\cos\theta + \tfrac{1}{2}H^{*2}S - UH^* - \frac{SU}{\cos\theta} + Q = 0. \tag{14}$$

In the special case $k = 0$ (corresponding to taking the thin-film limit $\epsilon \to 0$ and then the Bingham limit $\lambda \to 0$) we have $H^* \equiv H$ so that region 3 is absent and the

problem reduces to that when $\lambda = O(1)$ in the special case $\lambda = 0$, while in the special case $k = \infty$ (corresponding to taking the Bingham limit $\lambda \to 0$ and then the thin-film limit $\epsilon \to 0$) only regions 2 and 3 are present. Both H^* and h are independent of k. Moreover, equations (8) and (9) in the special case $\lambda = 0$ are equivalent to (11) and (12) when H is replaced by H^*, and so the solutions for the free surface h and the pseudo-yield surface H^* in the distinguished limit are identical to those for the free surface h and the yield surface H that are obtained by setting $\lambda = 0$ in the solution for $\lambda = O(1)$. Of course, this does not mean that other quantities (such as, for example, the stress) are the same. Setting $\lambda = 0$ in (10) confirms that in this case the solution in the unyielded zone is simply a rigid plug; we shall subsequently find that these occur only for flow on a rotating cylinder ($U \neq 0$). Note that, as in the case $\lambda = O(1)$, H^*, H and h depend on θ only through $\cos\theta$ and hence have top-to-bottom symmetry.

4. Stationary cylinder ($U = 0$) when $\lambda = O(1)$

In this section we consider the solution when $\lambda = O(1)$ as $\epsilon \to 0$ in the special case $U = 0$ corresponding to thin-film flow with prescribed volume flux Q round a stationary cylinder. For ease of comparison with the earlier work on this problem (and to distinguish between the present results and those for a rotating cylinder which follow) we present all the results for a stationary cylinder in terms of the local angle to the horizontal α (defined in § 3) instead of the polar angle θ. To obtain the appropriate equations from the general ones given in § 3 we set $U = 0$ and $\theta = \pi/2 - \alpha$ and replace u and Q with $-u$ and $-Q$ respectively. In this case, just as Nusselt (1916*a*, *b*) found in the Newtonian case, the only physically acceptable solution corresponds to a curtain of fluid falling onto the top ($\alpha = 0$) of and falling off at the bottom ($\alpha = \pi$) of the cylinder. When a flux Q_s of fluid is supplied from above the cylinder a portion Q will flow round the right-hand side ($0 < \alpha < \pi$) and the remainder $Q_s - Q$ will flow round the left-hand side ($-\pi < \alpha < 0$) of the cylinder. As Duffy & Wilson (1999) point out, the fluxes Q and $Q_s - Q$ need not be equal, and so the overall flow need not have left-to-right symmetry. However, without loss of generality we restrict our attention to flow round the right side of the cylinder in what follows; the corresponding flow on the left side can then be calculated in the same way with Q replaced by $Q_s - Q$.

Eliminating H between (8) and (9) gives a cubic polynomial equation for h in the yielded zone, namely

$$h^3 - \frac{3(1-\lambda)}{2\sin\alpha}h^2 + \frac{1-\lambda}{2\sin^3\alpha} - \frac{3Q}{\sin\alpha} = 0. \tag{15}$$

If we define

$$K = 1 - \frac{2}{(1-\lambda)^2} + \frac{12Q\sin^2\alpha}{(1-\lambda)^3} \tag{16}$$

then from (15) the only physically acceptable solution for the free surface h is

$$h = \begin{cases} \dfrac{1-\lambda}{2\sin\alpha}[1 + 2\cos(\frac{1}{3}\cos^{-1}K)], & -1 \leqslant K \leqslant 1, \\ \dfrac{1-\lambda}{2\sin\alpha}[1 + 2\cosh(\frac{1}{3}\cosh^{-1}K)], & K > 1. \end{cases} \tag{17}$$

The yield surface H is then given by (9), so that

$$H = h - \frac{1}{\sin\alpha}. \tag{18}$$

The edges of the yielded zone are where $H = 0$. Thus from (15) and (18) the yielded zone is $\alpha_e < \alpha < \pi - \alpha_e$, where α_e $(0 \leqslant \alpha_e \leqslant \pi/2)$ is given by

$$\alpha_e = \sin^{-1}\left[\left(\frac{\lambda}{3Q}\right)^{1/2}\right], \tag{19}$$

and so

$$h(\alpha_e) = \left(\frac{3Q}{\lambda}\right)^{1/2}. \tag{20}$$

Thus a yielded zone is present only if $Q > \lambda/3$.

In the unyielded zone we have from (10)

$$u = \tfrac{1}{2}\lambda \sin\alpha(2h - z)z, \quad h = \left(\frac{3Q}{\lambda \sin\alpha}\right)^{1/3}, \tag{21}$$

as given, for example, by Nusselt (1916*a*, *b*).

It can be shown that h takes its minimum value at $\alpha = \pi/2$ and increases monotonically away from $\alpha = \pi/2$, becoming infinite at $\alpha = 0$ and $\alpha = \pi$. H may have either a local maximum or a local minimum at $\alpha = \pi/2$; Ross (2000) gives further details. The fluid is always unyielded near $\alpha = 0$ and $\alpha = \pi$.

In the limit $Q \to 0$ the fluid is unyielded everywhere and the flow is described by (21). In the limit $Q \to \infty$ we have $\alpha_e = (\lambda/3Q)^{1/2} + O(Q^{-3/2})$ and

$$H = \left(\frac{3Q}{\sin\alpha}\right)^{1/3} - \frac{1+\lambda}{2\sin\alpha} + O(Q^{-1/3}), \tag{22}$$

$$h = \left(\frac{3Q}{\sin\alpha}\right)^{1/3} + \frac{1-\lambda}{2\sin\alpha} + O(Q^{-1/3}). \tag{23}$$

These two expansions are non-uniform when $\alpha = O(Q^{-1/2})$, that is, when α is of the same order as α_e. These non-uniformities are resolved by appropriate inner solutions in which H increases from zero at $\alpha = \alpha_e$ to the $O(Q^{1/3})$ value given in (22) and h decreases from the $O(Q^{1/2})$ value given in (20) at $\alpha = \alpha_e$ to the $O(Q^{1/3})$ value given in (23).

There are two distinct flow topologies in this case. If $Q \leqslant \lambda/3$ then the flow is unyielded everywhere (type I), while if $Q > \lambda/3$ then there is a yielded zone (type II); typical examples of these two different flows (with streamlines included) are shown in figure 3. In particular, figure 3(*b*) shows that some streamlines lie entirely in the unyielded region whereas others enter and exit the yielded region, confirming that the yield surface is not a material surface.

Figure 4 shows H and h plotted as functions of α/π for a range of values of λ when $Q = 1$. Note that only in the special case $\lambda = 0$ does the yielded zone extend all the way around the cylinder. In the special case $\lambda = 1$ the 'yield surface' H merely represents a surface in the fluid on which the stress takes the yield value of unity and the fluid undergoes no material change there since the viscosity is the same in the yielded and unyielded regions. Evidently h and h' are continuous but h'' is, in general, discontinuous at $\alpha = \alpha_e$; this discontinuity in h'' accounts for the lack of smoothness of the free surface at $\alpha = \alpha_e$ just evident in figure 3(*b*) and in figure 4 in the case $\lambda = 1/10$. Ross (2000) gives further details.

The solution in the special case $\lambda = 0$ is of particular interest. In this case the velocity in region 1 is simply $u_1 = H^2 \sin\alpha/2$, which varies with α but not z, and

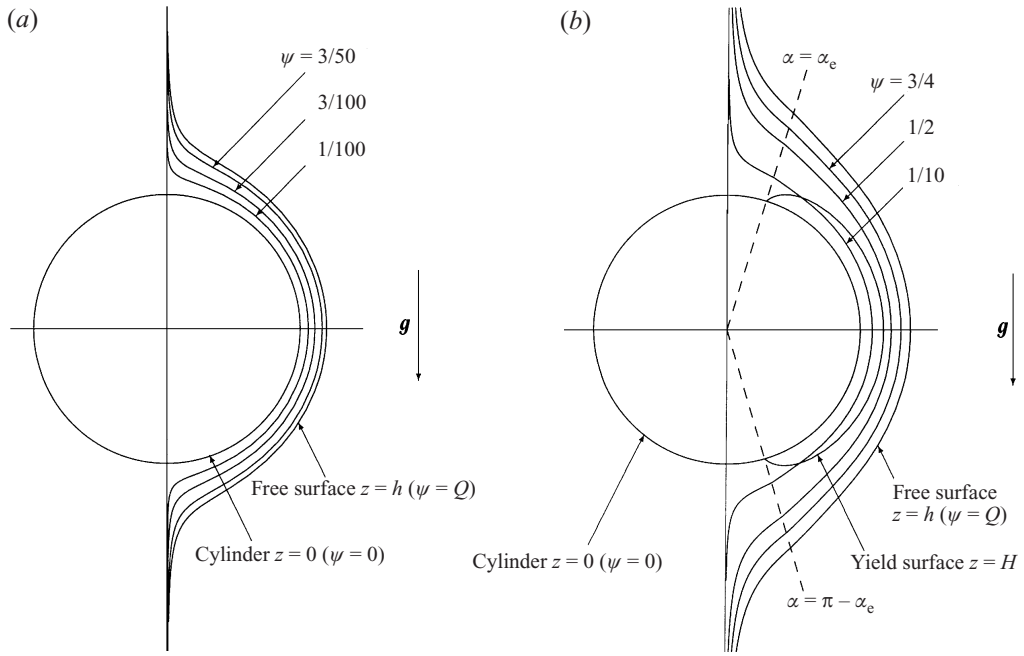

FIGURE 3. Leading-order solutions for flow round a large stationary cylinder (including typical streamlines on which the stream function ψ is constant) illustrating (*a*) a flow of type I when $Q = 2/25$ and $\lambda = 1/4$, and (*b*) a flow of type II when $Q = 1$ and $\lambda = 1/4$.

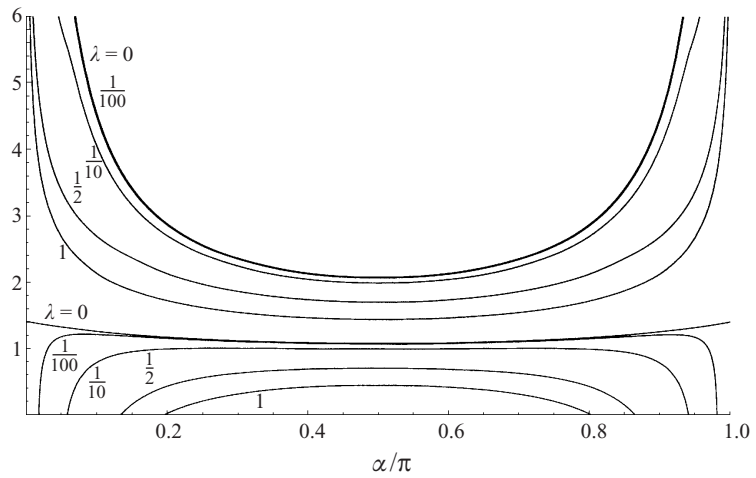

FIGURE 4. Plots of H (lower curves) and h (upper curves) as functions of α/π when $Q = 1$ for $\lambda = 0$, 1/100, 1/10, 1/2 and 1. Note that the solutions for h in the cases $\lambda = 0$ and $\lambda = 1/100$ are virtually indistinguishable at this scale.

$\alpha_e = 0$, that is, the unyielded zone is absent. We note that

$$H = (2Q)^{1/2} - \tfrac{2}{3}Q\,\alpha + O(\alpha^2), \tag{24}$$

$$h = \frac{1}{\alpha} + (2Q)^{1/2} + \tfrac{1}{6}(1 - 4Q)\alpha + O(\alpha^2) \tag{25}$$

as $\alpha \to 0$,

$$H = (2Q)^{1/2} - \tfrac{2}{3}\sin\alpha\, Q + O(Q^{3/2}), \tag{26}$$

$$h = \frac{1}{\sin\alpha} + (2Q)^{1/2} - \tfrac{2}{3}\sin\alpha\, Q + O(Q^{3/2}) \tag{27}$$

as $Q \to 0$, and (22) and (23) with $\lambda = 0$ hold as $Q \to \infty$.

5. Stationary cylinder ($U = 0$) when $k = O(1)$

In this section we consider the solution in the distinguished limit $\lambda \to 0$ and $\epsilon \to 0$ in which $k = \epsilon/\lambda = O(1)$ in the special case $U = 0$, corresponding to thin-film flow with prescribed volume flux Q round a stationary cylinder. From (11)–(13) in the yielded zone H^*, H and h satisfy

$$Q = \tfrac{1}{6}\sin\alpha(3h - H^*)H^{*2}, \tag{28}$$

$$(h - H^*)\sin\alpha = 1, \tag{29}$$

$$(h - H)^2\sin^2\alpha + k^2\left[\frac{\mathrm{d}}{\mathrm{d}\alpha}\{H^{*2}\sin\alpha\}\right]^2 = 1. \tag{30}$$

Using (29) to eliminate h from (28) yields

$$Q = \tfrac{1}{3}H^{*3}\sin\alpha + \tfrac{1}{2}H^{*2}. \tag{31}$$

The edges of the yielded zone are where $H^* = 0$, and are at $\alpha = \alpha_e^*$ and $\alpha = \pi - \alpha_e^*$, where α_e^* is identical to α_e in the case $\lambda = 0$. All the results for H, h and $\alpha_e(=0)$ in the case $\lambda = 0$ given in §4 apply directly to H^*, h and $\alpha_e^*(=0)$ in the present problem. Solving (30) yields

$$H = h - \frac{1}{\sin\alpha}\left[1 - \left(k\frac{\mathrm{d}}{\mathrm{d}\alpha}\{H^{*2}\sin\alpha\}\right)^2\right]^{1/2}, \tag{32}$$

where, from (31),

$$\frac{\mathrm{d}}{\mathrm{d}\alpha}\{H^{*2}\sin\alpha\} = \frac{(3 + H^*\sin\alpha)H^{*2}\cos\alpha}{3(1 + H^*\sin\alpha)}. \tag{33}$$

Note that $H^* = H$ when $\alpha = \pi/2$, and so region 3 is always absent at this special value of α.

Although H^* and h always extend from $\alpha = 0$ to $\alpha = \pi$, the same is not necessarily true for H; specifically, we find that if $Q > 1/2k$ then the yield surface H meets the free surface h at $\alpha = \alpha_e$ and $\alpha = \pi - \alpha_e$, where α_e ($0 \leqslant \alpha_e \leqslant \pi/2$) is the (unique) solution of $k\mathrm{d}\{H^{*2}\sin\alpha\}/\mathrm{d}\alpha = 1$. If $Q \leqslant 1/2k$ then

$$H = \begin{cases} \dfrac{1}{\alpha}[1 - (1 - 4k^2Q^2)^{1/2}] + (2Q)^{1/2}\left[1 - \dfrac{16k^2Q^2}{3(1 - 4k^2Q^2)^{1/2}}\right] + O(\alpha), & Q < \dfrac{1}{2k}, \\ \dfrac{1}{\alpha} - \dfrac{1}{k^{1/4}}\left(\dfrac{8}{3\alpha}\right)^{1/2} + \dfrac{1}{k^{1/2}} + O(\alpha^{1/2}), & Q = \dfrac{1}{2k}, \end{cases} \tag{34}$$

as $\alpha \to 0$, while if $Q > 1/2k$ then

$$H = h(\alpha_e) - \frac{(\alpha - \alpha_e)^{1/2}}{\sin\alpha_e}\left[-2k\frac{\mathrm{d}^2}{\mathrm{d}\alpha^2}\{H^{*2}\sin\alpha\}\right]_{\alpha=\alpha_e}^{1/2} + O(\alpha - \alpha_e) \tag{35}$$

as $\alpha \to \alpha_e^+$. All three surfaces always have a global minimum at $\alpha = \pi/2$.

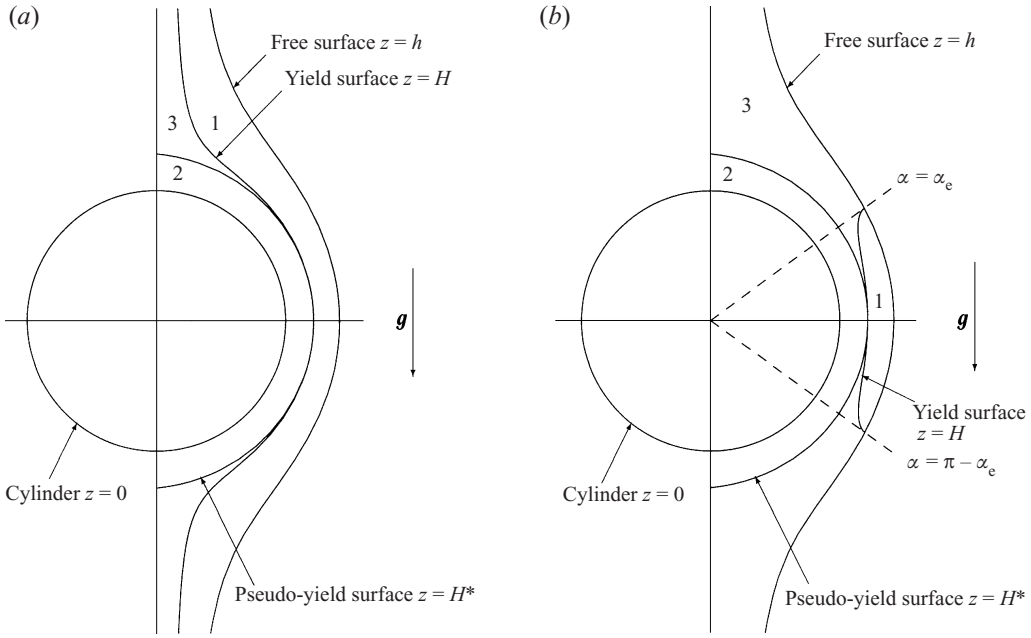

FIGURE 5. Leading-order solutions for flow round a large stationary cylinder in the distinguished limit described in § 5 illustrating (*a*) a flow of type II_1 when $Q = 1$ and $k = 9/20$, and (*b*) a flow of type II_2 when $Q = 1$ and $k = 2$.

There are two distinct flow topologies in this case. If $Q \leqslant 1/2k$ then there is only a partially yielded zone (type II_1), while if $Q > 1/2k$ then there are a partially yielded zone and two fully yielded zones (type II_2); typical examples of these two different flows are shown in figure 5. In particular, figure 5(*a*) shows that fluid particles start (at $\alpha = 0$) and finish (at $\alpha = \pi$) in the pseudo-plug (regions 1 and 3), but may pass through the yielded region (region 2), whilst figure 5(*b*) shows that all particles start and finish in region 3, but must, in general, pass through either region 1 or region 2. Figure 6 shows H^*, H and h plotted as functions of α/π for a range of values of k when $Q = 1$.

In the limit $k \to 0$ we have $H = H_0 + k^2 H_2 + O(k^4)$, where $H_0 = H^*$ and

$$H_2 = \frac{1}{2\sin\alpha}\left(\frac{\mathrm{d}}{\mathrm{d}\alpha}\{H^{*2}\sin\alpha\}\right)^2. \tag{36}$$

In particular, $H_2 = O(\alpha^{-1})$ as $\alpha \to 0$ and so this expansion is non-uniform when $\alpha = O(k^2)$. This non-uniformity is resolved by an appropriate inner solution near $\alpha = 0$; Ross (2000) gives details of this.

In the limit $k \to \infty$ we have

$$\alpha_{\mathrm{e}} = \frac{\pi}{2} - \frac{3(1+H_0^*)}{H_0^{*2}(3+H_0^*)}\frac{1}{k} + O(k^{-2}), \tag{37}$$

where $H_0^* = H^*(\pi/2)$, and the behaviour of H^*, H and h in the partially yielded zone

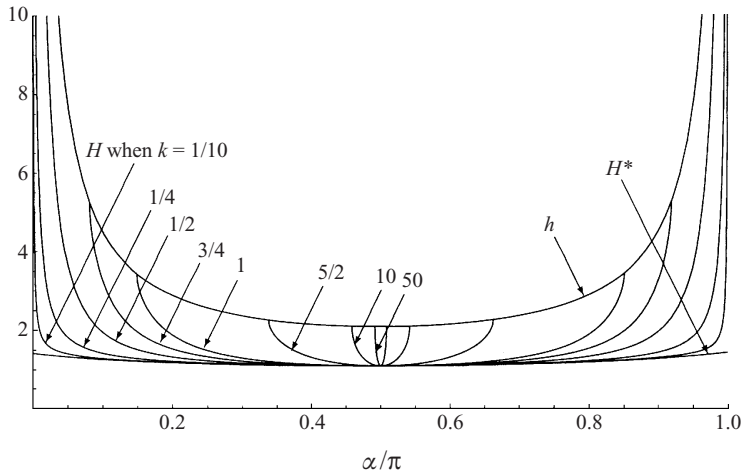

FIGURE 6. Plots of H^*, H and h as functions of α/π when $Q = 1$ for $k = 1/10$, $1/4$, $1/2$, $3/4$, 1, $5/2$, 10 and 50. Note that H^* and h are independent of k.

is given by $H^* = H_0^* + O(k^{-2})$,

$$H = 1 + H_0^* - \left[1 - \left(\frac{\frac{1}{2}\pi - \alpha}{\frac{1}{2}\pi - \alpha_e}\right)^2\right]^{1/2} + O(k^{-2}) \tag{38}$$

and $h = 1 + H_0^* + O(k^{-2})$. Thus at leading order h and H^* are constant (independent of α) whereas H has a semi-elliptical shape with width $O(k^{-1})$ and unit height.

In the limit $Q \to 0$ we find that H^* and h are given by (26) and (27) respectively and that H^* differs from H only at $O(Q^2)$. The solution for H (but not that for H^* or h) is non-uniform when $\alpha = O(Q^{1/2})$. This non-uniformity is resolved by an appropriate inner solution near $\alpha = 0$.

In the limit $Q \to \infty$ we find that H^* and h are given by (22) and (23) with $\lambda = 0$ respectively. Furthermore, $\alpha_e = \pi/2 - 3^{1/3}k^{-1}Q^{-2/3} + O(Q^{-1/2})$, and the behaviour of H^*, H and h in the partially yielded zone is given by $H^* = (3Q)^{1/3} - 1/2 + O(Q^{-1/3})$,

$$H = (3Q)^{1/3} + \frac{1}{2} - \left[1 - \left(\frac{\frac{1}{2}\pi - \alpha}{\frac{1}{2}\pi - \alpha_e}\right)^2\right]^{1/2} + O(Q^{-1/3}) \tag{39}$$

and $h = (3Q)^{1/3} + 1/2 + O(Q^{-1/3})$. Thus to first order H^* and h are constant (independent of α) whereas H has a semi-elliptical shape with width $O(Q^{-2/3})$ and unit height.

6. Rotating cylinder ($U \neq 0$) when $\lambda = O(1)$

In this section we consider the solution when $\lambda = O(1)$ as $\epsilon \to 0$ in the general case $U \neq 0$ corresponding to thin-film flow with volume flux Q round a rotating cylinder. In this case, just as Duffy & Wilson (1999) found in the Newtonian case, there are two physically acceptable solutions, one corresponding to a film of finite non-zero thickness everywhere (the solution studied in the Newtonian case by Moffatt 1977) and another corresponding to a curtain of fluid falling onto the top of and off at

the bottom of the cylinder (studied in the Newtonian case by Duffy & Wilson 1999). In this work we shall be concerned exclusively with the former solution. Note that this solution is absent in the special case $U = 0$ treated earlier, and so the following results do not, in general, reduce to those given in § 4 and § 5 in the limit $U \to 0$.

Eliminating H from (8) by using (9) gives a cubic polynomial equation for h in the yielded zone, namely

$$h^3 - \frac{3(1-\lambda)}{2|\cos\theta|}h^2 - \frac{3U}{\cos\theta}h + \frac{1-\lambda}{2|\cos\theta|^3} + \frac{3Q}{\cos\theta} = 0. \tag{40}$$

If we define

$$K = \frac{1}{|M|^{3/2}}[(1-\lambda)^3 - 2(1-\lambda)(1-3U\cos\theta) - 12SQ\cos^2\theta], \tag{41}$$

where $M = (1-\lambda)^2 + 4U\cos\theta$, then from (40) the appropriate solution for the free surface h is

$$h = \frac{1-\lambda}{2\cos\theta} + \frac{M^{1/2}}{\cos\theta}\cos(\tfrac{2}{3}\pi - \tfrac{1}{3}\cos^{-1}K), \quad -1 \leqslant K \leqslant 1, \tag{42}$$

on the right ($S = 1$), and

$$h = \begin{cases} \dfrac{1-\lambda}{2|\cos\theta|} + \dfrac{|M|^{1/2}}{|\cos\theta|}\sinh(\tfrac{1}{3}\sinh^{-1}K), & M \leqslant 0, \\ \dfrac{1-\lambda}{2|\cos\theta|} + \dfrac{M^{1/2}}{|\cos\theta|}\cos(\tfrac{1}{3}\cos^{-1}K), & M > 0 \quad \text{and} \quad -1 \leqslant K \leqslant 1, \\ \dfrac{1-\lambda}{2|\cos\theta|} + \dfrac{M^{1/2}}{|\cos\theta|}\cosh(\tfrac{1}{3}\cosh^{-1}K), & M > 0 \quad \text{and} \quad K > 1, \end{cases} \tag{43}$$

on the left ($S = -1$). The yield surface H is given by (9). Since H and h do not have left-to-right symmetry, hereafter the subscripts R and L will be used to denote quantities on the right ($S = 1$) and left ($S = -1$), respectively, when necessary. The solution (42) is physically sensible only if $K \geqslant -1$ throughout the yielded zone, and in particular if $K \geqslant -1$ at $\theta = 0$, that is, if $Q \leqslant Q_C$, where

$$Q_C = \tfrac{1}{12}[(1-\lambda)^3 - 2(1-\lambda)(1-3U) + [(1-\lambda)^2 + 4U]^{3/2}]. \tag{44}$$

It may be shown that $h' \leqslant 0$ for $0 \leqslant \theta \leqslant \pi$, so that τ takes its maximum value of $h(0)$ at $z = 0$, $\theta = 0$, and hence there can be a region of yielded fluid only if $h(0) > 1$. From (42) it is clear that $h(0)$ is maximized when $Q = Q_C$ (corresponding to $K = -1$), and a necessary condition for yielded zones to exist is therefore $U > \lambda$. For $U \leqslant \lambda$ the flow is unyielded everywhere.

As before, the edges of the yielded zone are where $H = 0$. Thus from (9) and (40) the yielded zones on the right and left are given by $|\theta| < \theta_{eR}$ and $|\pi - \theta| < \pi - \theta_{eL}$, respectively, where θ_{eR} ($0 \leqslant \theta_{eR} \leqslant \pi/2$) and θ_{eL} ($\pi/2 \leqslant \theta_{eL} \leqslant \pi$) are given by

$$\theta_e = \cos^{-1}\left[\frac{SU}{2Q}\left(1 + \left\{1 - \frac{4S\lambda Q}{3U^2}\right\}^{1/2}\right)\right], \tag{45}$$

and so

$$h(\theta_e) = \frac{3SU}{2\lambda}\left(1 - \left\{1 - \frac{4S\lambda Q}{3U^2}\right\}^{1/2}\right), \tag{46}$$

with the appropriate choice for S. Thus from (45) a yielded zone is present on the right only if

$$Q \leqslant \frac{3U^2}{4\lambda}, \quad Q > \tfrac{1}{2}U, \quad Q > Q_{\mathrm{R}}, \tag{47}$$

where

$$Q_{\mathrm{R}} = U - \tfrac{1}{3}\lambda. \tag{48}$$

Similarly, from (45) a yielded zone is present on the left only if $Q > Q_{\mathrm{L}}$, where

$$Q_{\mathrm{L}} = U + \tfrac{1}{3}\lambda \geqslant Q_{\mathrm{R}}. \tag{49}$$

From (45) we find that $\theta_{\mathrm{eR}} \geqslant \pi - \theta_{\mathrm{eL}}$ (with equality when $\lambda = 0$) and so the extent of the yielded zone is always greater on the right than on the left when $\lambda \neq 0$.

From (10) h in the unyielded zone satisfies

$$h^3 - \frac{3U}{\lambda\cos\theta}h + \frac{3Q}{\lambda\cos\theta} = 0. \tag{50}$$

If we define

$$K_{\mathrm{N}} = -\frac{3SQ}{2}\left(\frac{\lambda|\cos\theta|}{U^3}\right)^{1/2} \tag{51}$$

then from (50) the appropriate solution for h is

$$h = 2\left(\frac{U}{\lambda\cos\theta}\right)^{1/2}\cos\left(\tfrac{2}{3}\pi - \tfrac{1}{3}\cos^{-1}K_{\mathrm{N}}\right), \quad -1 \leqslant K_{\mathrm{N}} \leqslant 0, \tag{52}$$

on the right ($S = 1$), and

$$h = 2\left(\frac{U}{\lambda|\cos\theta|}\right)^{1/2}\sinh\left(\tfrac{1}{3}\sinh^{-1}K_{\mathrm{N}}\right), \quad K_{\mathrm{N}} > 0, \tag{53}$$

on the left ($S = -1$). If the fluid is unyielded everywhere then (52) is physically sensible only if $Q \leqslant Q_{\mathrm{N}}$, where $Q_{\mathrm{N}} = 2U^{3/2}/3\lambda^{1/2}$, in agreement with Moffatt's (1977) result in the Newtonian case.

It can be shown that h takes its maximum value at $\theta = 0$ and decreases monotonically away from $\theta = 0$ to its minimum value at $\theta = \pi$. H always has a local maximum at $\theta = 0$ but may have either a local maximum or a local minimum at $\theta = \pi$; Ross (2000) gives further details. The flow is always unyielded near $\theta = \pm\pi/2$ where $h = Q/U$.

As we have seen, yielded zones can exist only for $U > \lambda$ and in this case the strongest restrictions on Q are $Q > Q_{\mathrm{R}}$, $Q \leqslant Q_{\mathrm{C}}$ and $Q > Q_{\mathrm{L}}$. For $U > \lambda$ we have $Q_{\mathrm{R}} < Q_{\mathrm{C}} < Q_{\mathrm{N}}$, with $Q_{\mathrm{R}} = Q_{\mathrm{C}} = Q_{\mathrm{N}} = 2\lambda/3$ when $U = \lambda$. There are therefore three distinct flow topologies. If $U \leqslant \lambda$ and $Q \leqslant Q_{\mathrm{N}}$ or $U > \lambda$ and $Q \leqslant Q_{\mathrm{R}}$ then the flow is unyielded everywhere (type I), if $U > \lambda$ and $Q_{\mathrm{R}} < Q \leqslant \min(Q_{\mathrm{C}}, Q_{\mathrm{L}})$ then there is a yielded zone on the right but not on the left (type II), while if $U > \lambda$ and $Q_{\mathrm{L}} < Q \leqslant Q_{\mathrm{C}}$ then there are yielded zones on both the right and left (type III); typical examples of these three different flows (with streamlines included) are shown in figure 7. Note that these definitions differ from those in § 4. Figure 8 shows a plot of a typical (U, Q) parameter plane for a fixed value of λ (in this case $\lambda = 1/2$); in particular it shows how the curves $Q = Q_{\mathrm{N}}$, $Q = Q_{\mathrm{R}}$, $Q = Q_{\mathrm{L}}$ and $Q = Q_{\mathrm{C}}$ divide the parameter plane into a region where no solution exists and regions in which the three different types of flow occur.

Figure 9 shows H and h plotted as functions of θ/π for a range of values of λ

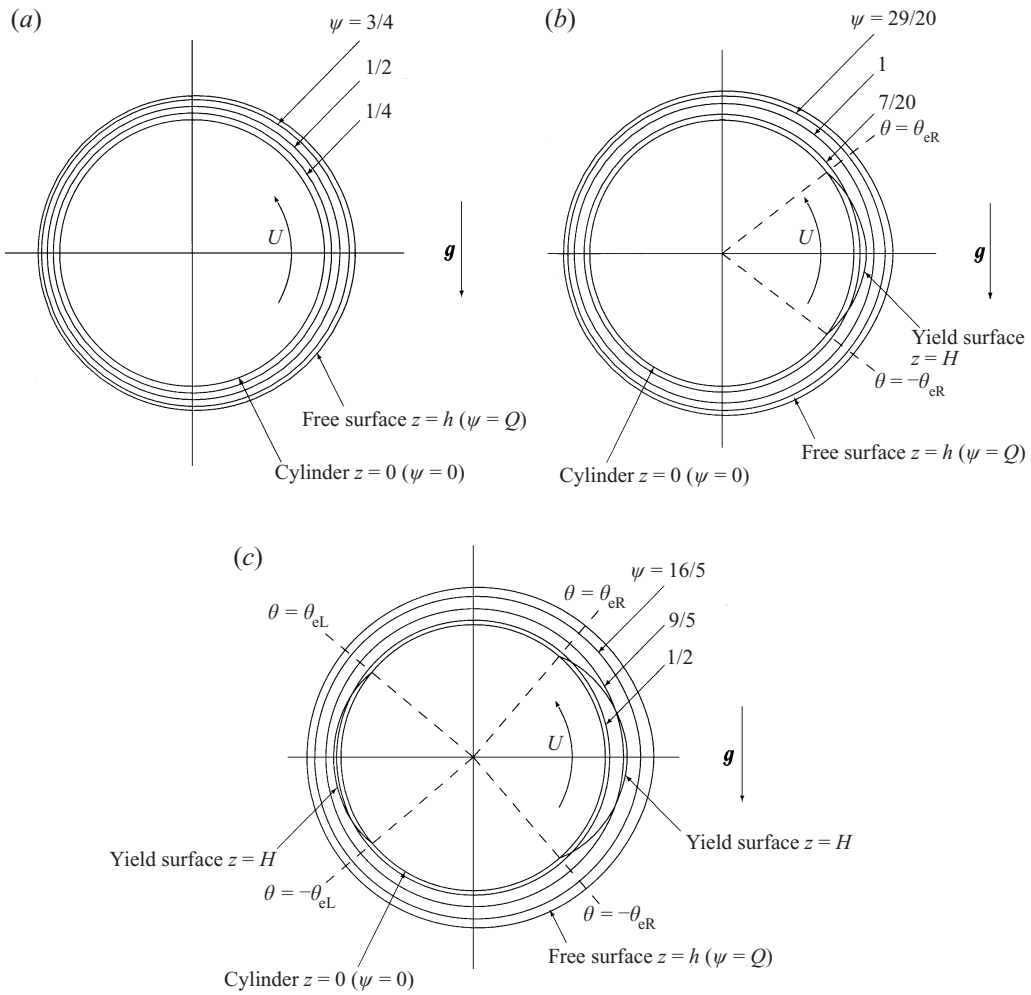

FIGURE 7. Leading-order solutions for flow round a large rotating cylinder (including typical streamlines on which the stream function ψ is constant) illustrating (*a*) a flow of type I when $Q = 9/10$, $\lambda = 1/2$ and $U = 1$, (*b*) a flow of type II when $Q = 7/4$, $\lambda = 1/2$ and $U = 8/5$, and (*c*) a flow of type III when $Q = 21/5$, $\lambda = 1/2$ and $U = 3$.

when $U = 19/10$ and $Q = 2$. Evidently, as in the case $U = 0$ discussed in § 4, h and h' are continuous but h'' is, in general, discontinuous at $\theta = \theta_e$.

Also of interest is the formation of corners in both H and h at $\theta = 0$ when $Q = Q_C$, shown in figure 9. When $Q = Q_C$ we find that H and h are given by $H = H_0 \mp A\theta + H_2\theta^2 + O(\theta^3)$ and $h = h_0 \mp A\theta + h_2\theta^2 + O(\theta^3)$ near $\theta = 0$, where

$$A = \left[\frac{h_0^3 + \lambda - 1}{3(2h_0 + \lambda - 1)}\right]^{1/2}, \quad h_2 = \frac{3h_0^2 - 2A^2}{6(2h_0 + \lambda - 1)}, \tag{54}$$

and where from (9) and (42) we have $H_0 = h_0 - 1$, $H_2 = h_2 - 1/2$ and

$$h_0 = \tfrac{1}{2}[1 - \lambda + ((1 - \lambda)^2 + 4U)^{1/2}], \tag{55}$$

showing that the profiles for both H and h have a corner at $\theta = 0$ with internal angle $\pi - 2A$ in this case. As $U \to \lambda^+$ we have $\theta_{eR} \to 0^+$, so that the extent of the yielded

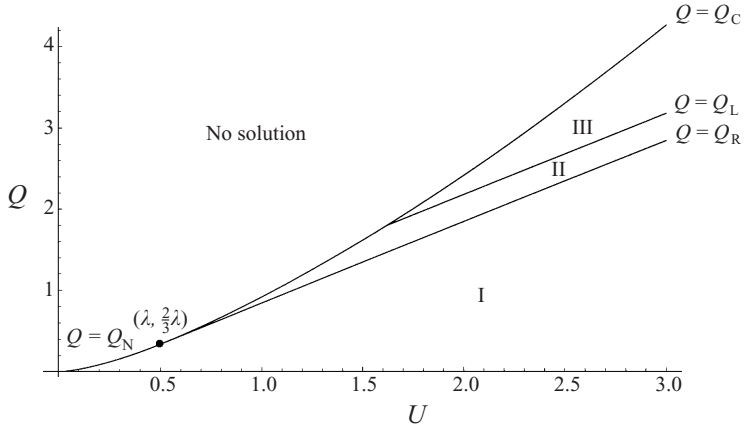

FIGURE 8. Plot of the (U, Q) parameter plane for the case $\lambda = 1/2$ showing how the curves $Q = Q_N$, $Q = Q_R$, $Q = Q_L$ and $Q = Q_C$ divide the parameter plane into regions in which either there is no solution or the flow is of type I, II or III.

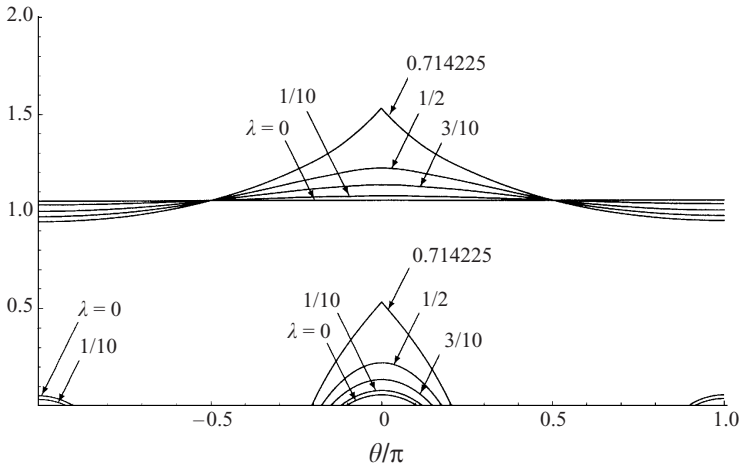

FIGURE 9. Plots of H (lower curves) and h (upper curves) as functions of θ/π when $U = 19/10$ and $Q = 2$ for $\lambda = 0$, $1/10$, $3/10$ ($Q = Q_L$), $1/2$ and 0.714225 ($Q = Q_C$).

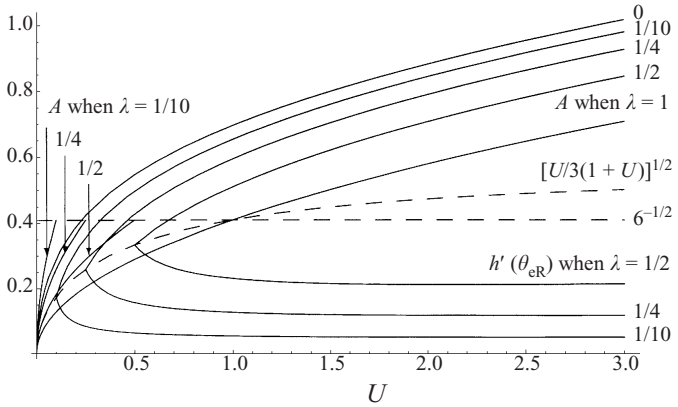

FIGURE 10. Plots of A and $h'(\theta_{eR})$ as functions of U for a range of values of λ. The curve $[U/3(1+U)]^{1/2}$ and the constant value $6^{-1/2}$ are shown with dashed lines.

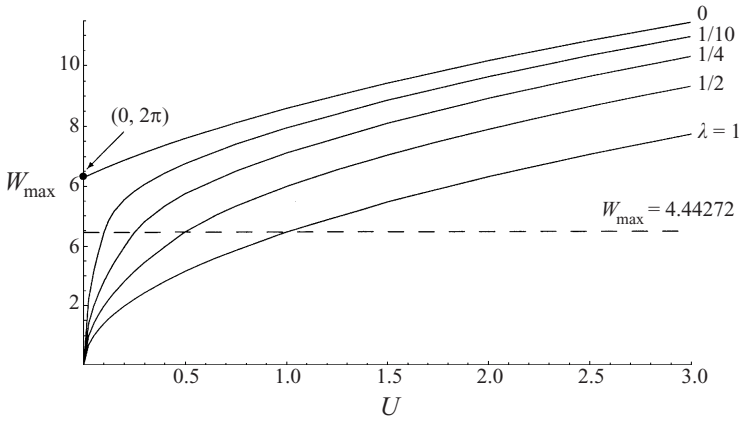

FIGURE 11. Plot of the maximum supportable weight on the cylinder $W_{\max}$ as a function of U for a range of values of λ. The constant value $W_{\mathrm{M}} \simeq 4.44272$ is shown with a dashed line.

zone on the right decreases to zero. Both A and $h'(\theta_{\mathrm{eR}})$ take the value $[U/3(1+U)]^{1/2}$ at $U = \lambda$. When $U \leqslant \lambda$ and $Q = Q_{\mathrm{N}}$ (in which case the flow is unyielded everywhere) h has a corner at $\theta = 0$ with $A = (U/6\lambda)^{1/2}$, in agreement with the result for a Newtonian fluid (see, for example, Duffy & Wilson 1999). Hence for $\lambda \neq 1$ there is a finite jump in the value of A from $6^{-1/2}$ to $[U/3(1+U)]^{1/2}$ at $U = \lambda$. Figure 10 shows A and $h'(\theta_{\mathrm{eR}})$ plotted as functions of U for a range of values of λ and, in particular, shows this jump. The special case $\lambda = 0$ is discussed later.

One property of considerable practical interest is the maximum weight of fluid that can be supported on the rotating cylinder (first considered by Moffatt 1977 in the Newtonian case). To leading order the weight of fluid on the cylinder is given by

$$W(\lambda, U, Q) = \int_0^{2\pi} h(\theta)\,\mathrm{d}\theta. \tag{56}$$

Just as Moffatt (1977) found in the Newtonian case W increases monotonically (almost, but not exactly, linearly) with Q until it reaches the maximum supportable weight $W_{\max}$. This maximum weight is given by $W_{\max} = W(\lambda, U, Q_{\mathrm{N}})$ when $U \leqslant \lambda$ and $W_{\max} = W(\lambda, U, Q_{\mathrm{C}})$ when $U > \lambda$. Figure 11 shows a plot of $W_{\max}$ as a function of U for a range of values of λ; in particular it shows that, for a given value of U, $W_{\max}$ for a viscoplastic material ($\lambda < 1$) always exceeds $W_{\max}$ for a Newtonian fluid ($\lambda = 1$), and that $W_{\max}$ is greatest for a Bingham material ($\lambda = 0$). Moreover, the maximum weight satisfies $W_{\max} \leqslant W_{\mathrm{M}}$ when $U \leqslant \lambda$ (i.e. when the flow is of type I) and $W_{\max} > W_{\mathrm{M}}$ when $U > \lambda$ (i.e. when the flow is of type II or III), where $W_{\mathrm{M}} \simeq 4.44272$ is the (corrected) value obtained by Moffatt (1977) (see, for example, Duffy & Wilson 1999).

The special case $\lambda = 0$ is again of particular interest. In this case the velocity in region 1 is simply $u_1 = U - H^2 \cos\theta/2$, which again varies with θ but not z. From (45) we have simply

$$\theta_{\mathrm{e}} = \cos^{-1}\left[\frac{SU}{Q}\right], \tag{57}$$

and thus $\theta_{\mathrm{eR}} = \pi - \theta_{\mathrm{eL}}$ and so the extents of the yielded zones on the right and the left are the same. From (44), (48) and (49) we obtain

$$Q_{\mathrm{C}} = \tfrac{1}{12}[6U - 1 + (1+4U)^{3/2}], \quad Q_{\mathrm{R}} = Q_{\mathrm{L}} = U. \tag{58}$$

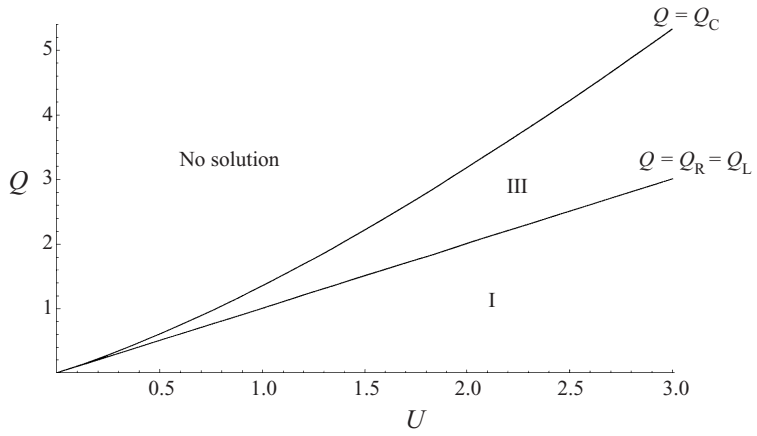

FIGURE 12. Plot of the (U, Q) parameter plane for the case $\lambda = 0$ showing how the curves $Q = Q_R = Q_L$ and $Q = Q_C$ divide the parameter plane into regions in which either there is no solution or the flow is of type I or III.

In the unyielded zone we have simply $u = U$ and $h = Q/U$, that is, a rigid plug of uniform thickness Q/U moving with constant speed U. Since $Q_R = Q_L$ flows of type II do not occur in this case. Figure 12 shows how the curves $Q = Q_R = Q_L$ and $Q = Q_C$ divide the (U, Q) parameter plane in this case into a region where no solution exists and regions in which flows of type I and III occur. Note that $h'(\theta_e) = 0$,

$$H'(\theta_e) = -\frac{S \sin\theta_e}{\cos^2\theta_e} = -\frac{SQ}{U^2}(Q^2 - U^2)^{1/2}, \tag{59}$$

and

$$H''(\theta_e) = \frac{Q}{U^5}(U^4 - SQU^2 - 2Q^2U^2 + SQ^3). \tag{60}$$

Figure 10 includes a plot of A as a function of U when $\lambda = 0$. Figure 11 includes a plot of W_{max} as a function of U when $\lambda = 0$; in particular, as $U \to 0$ the solution approaches a rigid plug of thickness unity all the way round the cylinder and so $W_{max} \to 2\pi$.

7. Rotating cylinder ($U \neq 0$) when $k = O(1)$

In this section we consider the solution in the distinguished limit $\lambda \to 0$ and $\epsilon \to 0$ in which $k = \epsilon/\lambda = O(1)$, in the general case $U \neq 0$ corresponding to thin-film flow with volume flux Q round a rotating cylinder. In the yielded zone H^*, H and h satisfy (11)–(13), and using (12) to eliminate h from (11) yields (14). The edges of the yielded zone are where $H^* = 0$, and are given by $|\theta| = \theta^*_{eR}$ and $|\pi - \theta| = \pi - \theta^*_{eL}$, where θ^*_{eR} and θ^*_{eL} are identical to θ_{eR} and θ_{eL} in the case $\lambda = 0$. All the results for H, h and θ_e in the case $\lambda = 0$ given in §6 apply directly to H^*, h and θ^*_e in the present problem. Solving (13) yields

$$H = h - \frac{1}{|\cos\theta|}\left[1 - \left(k\frac{\mathrm{d}}{\mathrm{d}\theta}\{H^{*2}\cos\theta\}\right)^2\right]^{1/2}, \tag{61}$$

where, from (14),

$$\frac{\mathrm{d}}{\mathrm{d}\theta}\{H^{*2}\cos\theta\} = \frac{H^*\sin\theta\,(H^{*3}\cos^2\theta + 3SH^{*2}\cos\theta - 3UH^*\cos\theta - 6SU)}{3\cos\theta\,(U - SH^* - H^{*2}\cos\theta)}, \tag{62}$$

except at $\theta = 0$ in the case $Q = Q_C$. As in the case $\lambda = O(1)$ considered in § 6, H^*, H and h do not have left-to-right symmetry. Note that $H^* = H$ at $\theta = 0$ for $Q \neq Q_C$, at $\theta = \pi$ and at the edges of the yielded zones, and so region 3 is always absent at these special values of θ.

When $Q_R < Q < Q_C$ there are two critical values of k, denoted by k_{critR} and k_{critL} ($> k_{critR}$), such that if $k \geqslant k_{critR}$ then H meets h at $\theta = \pm\theta_{e1R}$ and $\theta = \pm\theta_{e2R}$ ($0 \leqslant \theta_{e1R} \leqslant \theta_{e2R} \leqslant \pi/2$) on the right, and if $k \geqslant k_{critL}$ then H meets h at $\theta = \pm\theta_{e1L}$ and $\theta = \pm\theta_{e2L}$ ($\pi/2 \leqslant \theta_{e2L} \leqslant \theta_{e1L} \leqslant \pi$) on the left, where θ_{e1} and θ_{e2} are the appropriate solutions of

$$k\frac{\mathrm{d}}{\mathrm{d}\theta}\{H^{*2}\cos\theta\} = 1. \tag{63}$$

As $\theta \to \theta_e^*$ from below (above) on the right (left) respectively we have

$$H = H_1(\theta - \theta_e^*) + H_2(\theta - \theta_e^*)^2 + O(\theta - \theta_e^*)^3, \tag{64}$$

where $H_1 = H_1^* = H^{*\prime}(\theta_e^*)$ is given by (59) and

$$H_2 = H_2^* + \frac{2Q^3k^2}{U^7}(Q^2 - U^2)^2, \tag{65}$$

where $H_2^* = H^{*\prime\prime}(\theta_e^*)/2$ is given by (60). If $k > k_{crit}$ then

$$H = h(\theta_{e1}) - \frac{S(-S(\theta - \theta_{e1}))^{1/2}}{\cos\theta_{e1}}\left[2Sk\frac{\mathrm{d}^2}{\mathrm{d}\theta^2}\{H^{*2}\cos\theta\}\right]_{\theta=\theta_{e1}}^{1/2} + O(\theta - \theta_{e1}) \tag{66}$$

as $\theta \to \theta_{e1}$ from below (above) on the right (left) respectively, and

$$H = h(\theta_{e2}) - \frac{S(S(\theta - \theta_{e2}))^{1/2}}{\cos\theta_{e2}}\left[-2Sk\frac{\mathrm{d}^2}{\mathrm{d}\theta^2}\{H^{*2}\cos\theta\}\right]_{\theta=\theta_{e2}}^{1/2} + O(\theta - \theta_{e2}) \tag{67}$$

as $\theta \to \theta_{e2}$ from above (below) on the right (left) respectively.

There are four distinct flow topologies in this case. If $Q \leqslant Q_R$ then the flow is of type I (a rigid plug of thickness Q/U), if $Q_R < Q < Q_C$ and $k < k_{critR}$ then the flow is of type III with only partially yielded zones on both the right and left (type III_1), if $Q_R < Q < Q_C$ and $k_{critR} < k < k_{critL}$ then the flow is of type III with both partially and fully yielded zones on the right but only a partially yielded zone on the left (type III_2), while if $Q_R < Q < Q_C$ and $k > k_{critL}$ then the flow is of type III with both partially and fully yielded zones on both the right and left (type III_3); typical examples of these different flows of type III are shown in figure 13. Figure 14 shows H^*, H and h plotted as functions of θ/π for a range of values of k for a value of Q satisfying $Q_R < Q < Q_C$.

In the special case $Q = Q_C$ we find that if $k \geqslant k_{critR}$ ($= 1/2H_0^*A$ when $Q = Q_C$) then H meets h at $\theta = \pm\theta_{e1R}$ ($0 \leqslant \theta_{e1R} \leqslant \pi/2$) on the right, where θ_{e1R} is the (unique) solution of (63); the behaviour on the left is as before. Note that, unlike when $k > k_{critR}$ for $Q_R < Q < Q_C$, H meets h only twice (as opposed to four times) when $k > k_{critR}$ for $Q = Q_C$. For $k < k_{critR}$ H is given by

$$H = 1 + H_0^* - [1 - (2H_0^*Ak)^2]^{1/2} \mp B\theta + O(\theta^2) \tag{68}$$

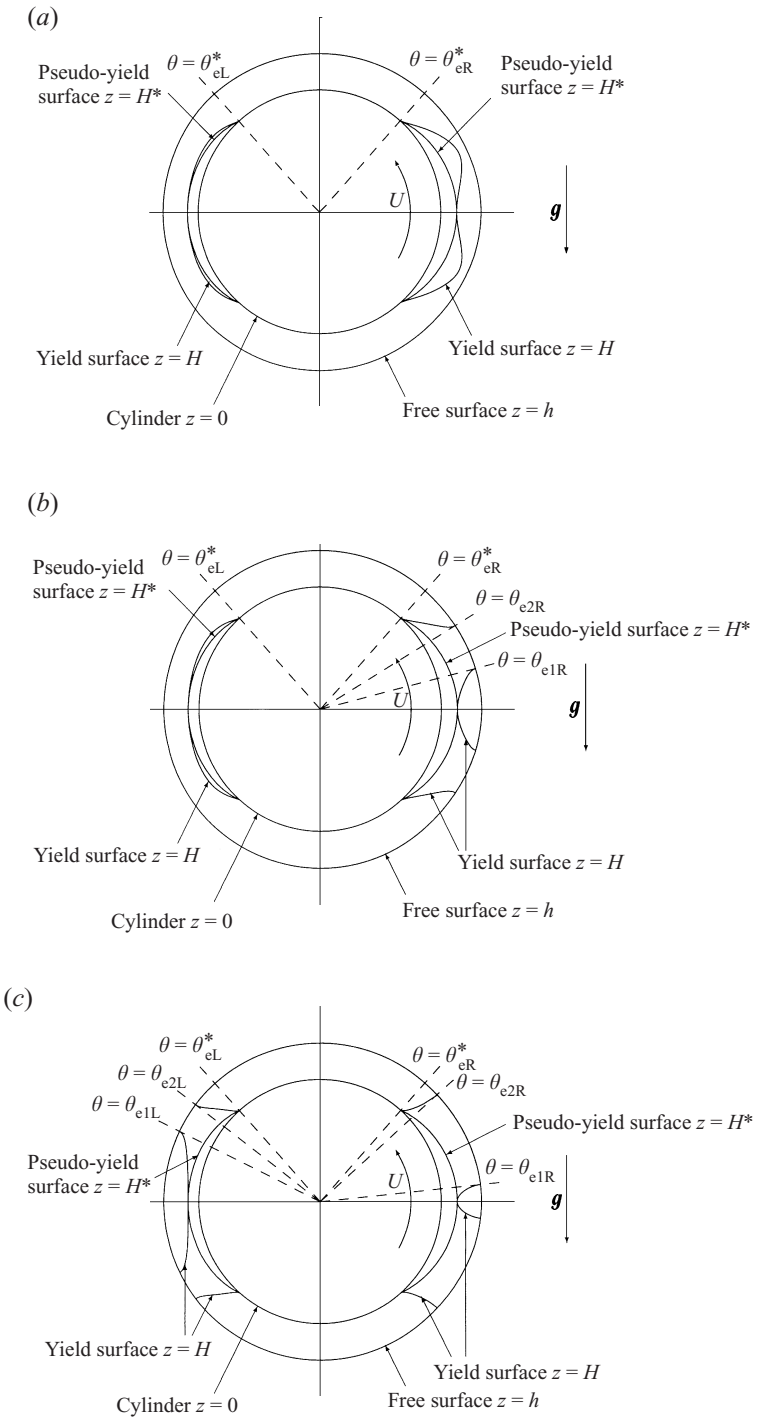

FIGURE 13. Leading-order solutions for flow round a large rotating cylinder in the distinguished limit described in § 7 illustrating (*a*) a flow of type III_1 when $U = 2$, $Q = 3$ and $k = 5/4$, (*b*) a flow of type III_2 when $U = 2$, $Q = 3$ and $k = 3/2$, and (*c*) a flow of type III_3 when $U = 2$, $Q = 3$ and $k = 3$.

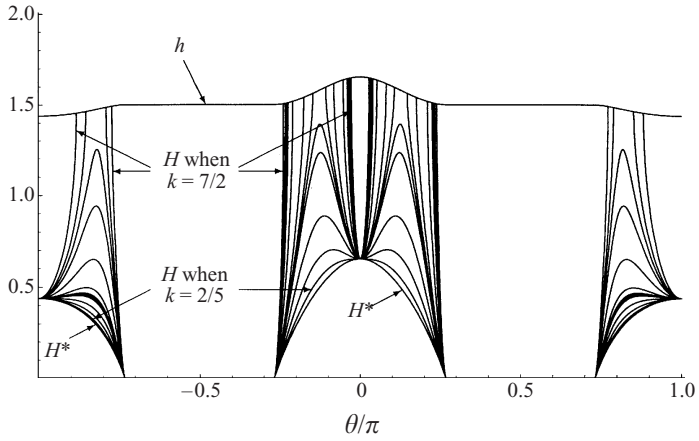

FIGURE 14. Plots of H^*, H and h as functions of θ/π when $U = 2$ and $Q = 3$ (so that $Q_R < Q < Q_C$) for $k = 2/5$, $7/10$, 1, $5/4$, $13/10$, $27/20$, $3/2$, 2, $5/2$, $11/4$, 3 and $7/2$. Note that H^* and h are independent of k.

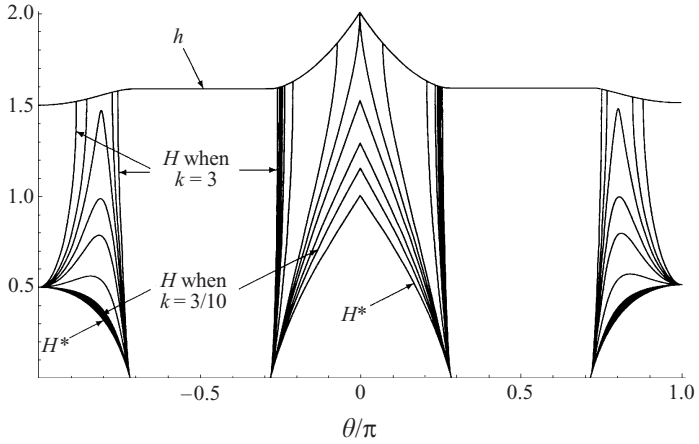

FIGURE 15. Plots of H^*, H and h as functions of θ/π when $U = 2$ and $Q = 19/6\,(= Q_C)$ for $k = 3/10$, $2/5$, $1/2$, $0.566947\,(= k_{critR})$, $13/20$, $5/4$, $7/4$, 2, $9/4$, $5/2$ and 3. Note that H^* and h are independent of k.

near $\theta = 0$, where

$$B = A - \frac{2H_0^* Ak^2(H_0^{*2} - 2A^2 - 4H_0^* H_2^*)}{[1 - (2H_0^* Ak)^2]^{1/2}}, \tag{69}$$

showing that the profile for H has a corner at $\theta = 0$ with internal angle $\pi - 2B$ in this case. In particular, $B \to \infty$ as $k \to k_{critR}^-$, that is, the corner becomes a cusp as it approaches the free surface. Furthermore (unlike in the case $Q_R < Q < Q_C$) $H \neq H^*$ at $\theta = 0$ for $Q = Q_C$. Figure 15 shows H^*, H and h plotted as functions of θ/π for a range of values of k in the case $Q = Q_C$.

In the limit $k \to 0$ we have $H = H_0 + k^2 H_2 + O(k^4)$, where $H_0 = H^*$ and

$$H_2 = \frac{1}{2|\cos\theta|}\left(\frac{\mathrm{d}}{\mathrm{d}\theta}\{H^{*2}\cos\theta\}\right)^2. \tag{70}$$

In contrast to the corresponding small-k solution in the case $U = 0$ described in § 5 this solution is uniform.

In the limit $k \to \infty$ when $Q_R < Q < Q_C$ we have

$$\theta_{e1R} = \frac{3(U - H_0^* - H_0^{*2})}{H_0^*(H_0^{*3} + 3H_0^{*2} - 3UH_0^* - 6U)}\frac{1}{k} + O(k^{-2}), \tag{71}$$

where $H_0^* = H^*(0)$, and the behaviour of H^*, H and h in the partially yielded zone $|\theta| \leqslant \theta_{e1R}$ is given by $H^* = H_0^* + O(k^{-2})$,

$$H = 1 + H_0^* - \left[1 - \left(\frac{\theta}{\theta_{e1R}}\right)^2\right]^{1/2} + O(k^{-2}) \tag{72}$$

and $h = 1 + H_0^* + O(k^{-2})$, analogous to the corresponding large-k solution in the case $U = 0$ described in § 5. Similarly when $Q_R < Q \leqslant Q_C$ we also have

$$\theta_{e1L} = \pi - \frac{3(U + H_0^* + H_0^{*2})}{H_0^*(H_0^{*3} + 3H_0^{*2} + 3UH_0^* + 6U)}\frac{1}{k} + O(k^{-2}), \tag{73}$$

where $H_0^* = H^*(\pi)$, and the behaviour of H^*, H and h in the partially yielded zone $|\pi - \theta| \leqslant \pi - \theta_{e1L}$ is given by $H^* = H_0^* + O(k^{-2})$,

$$H = 1 + H_0^* - \left[1 - \left(\frac{\pi - \theta}{\pi - \theta_{e1L}}\right)^2\right]^{1/2} + O(k^{-2}) \tag{74}$$

and $h = 1 + H_0^* + O(k^{-2})$, again analogous to the corresponding large-k solution in the case $U = 0$ described in § 5. Moreover,

$$\theta_{e2} = \theta_e^* - \frac{\cos^3\theta_e^*}{2\sin^2\theta_e^*}\frac{1}{k} + O(k^{-2}), \tag{75}$$

and the behaviour of H^*, H and h in the partially yielded zones $\theta_{e2R} \leqslant \theta \leqslant \theta_{eR}^*$ and $\theta_{eL}^* \leqslant \theta \leqslant \theta_{e2L}$ is given by $H^* = O(k^{-1})$,

$$H = \frac{1}{|\cos\theta_e^*|}\left[1 - \left(1 - \left\{\frac{\theta_e^* - \theta}{\theta_e^* - \theta_{e2}}\right\}^2\right)^{1/2}\right] + O(k^{-1}) \tag{76}$$

and $h = 1/|\cos\theta_e^*| + O(k^{-2})$. Thus at leading order h and H^* are constant (independent of θ) whereas H has a semi-elliptical shape with width $O(k^{-1})$ and height $1/|\cos\theta_e^*|$. The solution for H (but not for H^* or h) is non-uniform when $\theta - \theta_e^* = O(k^{-2})$. This non-uniformity is resolved by an appropriate inner solution near $\theta = \theta_e^*$ satisfying $H'(\theta_e^*) = H^{*\prime}(\theta_e^*)$.

8. Conclusions

In this paper we considered the steady two-dimensional thin-film flow of a viscoplastic material, modelled as a biviscosity fluid with a yield stress, round the outside of a large horizontal stationary or rotating cylinder. In both cases we determined the leading-order solution both when $\lambda = O(1)$ as $\epsilon \to 0$ and in the distinguished limit $\lambda \to 0$ and $\epsilon \to 0$ in which $k = \epsilon/\lambda = O(1)$. When $\lambda = O(1)$ the flow consists, in general, of a region of yielded fluid (region 2) adjacent to the cylinder and a region of unyielded fluid (region 1) adjacent to the free surface, separated by $z = H$. In the

distinguished limit the flow consists, in general, of a region of yielded fluid (region 2) adjacent to the cylinder whose stress is $O(1)$ above the yield stress and a pseudo-plug region adjacent to the free surface, in which the leading-order azimuthal component of velocity varies azimuthally but not radially, separated by $z = H^*$; the pseudo-plug is itself, in general, divided by $z = H$ into a region of yielded fluid (region 3) whose stress is $O(\epsilon)$ above the yield stress and a region of unyielded fluid (region 1) adjacent to the free surface.

The solution for a stationary cylinder represents a curtain of fluid with prescribed volume flux Q falling onto the top of and off at the bottom of the cylinder. If $Q \leqslant \lambda/3$ then the flow is unyielded everywhere (type I), but when $Q > \lambda/3$ there is a yielded zone (type II). In the distinguished limit region 2 always extends all the way round the cylinder, but region 1 does so only when $Q \leqslant 1/2k$.

For a rotating cylinder a solution representing a film with finite thickness everywhere is possible only when the flux is sufficiently small. If $U \leqslant \lambda$ and $Q \leqslant Q_{\mathrm{N}}$ or $U > \lambda$ and $Q \leqslant Q_{\mathrm{R}}$ then the flow is unyielded everywhere (type I), if $U > \lambda$ and $Q_{\mathrm{R}} < Q \leqslant \min(Q_{\mathrm{C}}, Q_{\mathrm{L}})$ then there is a yielded zone on the right but not on the left (type II), while if $U > \lambda$ and $Q_{\mathrm{L}} < Q \leqslant Q_{\mathrm{C}}$ then there are yielded zones on both the right and left (type III). At the critical maximum flux ($Q = Q_{\mathrm{N}}$ when $U \leqslant \lambda$ and $Q = Q_{\mathrm{C}}$ when $U > \lambda$) the maximum supportable weight of fluid on the cylinder is attained and H^*, H and h all have a corner at $\theta = 0$. In the distinguished limit we have $Q_{\mathrm{R}} = Q_{\mathrm{L}}$ (so that flows of type II do not occur) and there are rigid plugs (absent in the stationary case) near the top and bottom of the cylinder.

All three authors gratefully acknowledge invaluable discussions with Dr S. D. R. Wilson (Department of Mathematics, University of Manchester) during the course of the present work. The first author (A. B. R.) wishes to express his gratitude to the Carnegie Trust for the Universities of Scotland for their financial support via a Carnegie Scholarship.

REFERENCES

Balmforth, N. J. & Craster, R. V. 1999 A consistent thin-layer theory for Bingham plastics. *J. Non-Newtonian Fluid Mech.* **84**, 65–81.

Barnes, H. A. 1999 The yield stress – a review or '$\pi\alpha\nu\tau\alpha\ \rho\epsilon\iota$' – everything flows? *J. Non-Newtonian Fluid Mech.* **81**, 133–178.

Beverly, C. R. & Tanner, R. I. 1992 Numerical analysis of three-dimensional Bingham plastic flow. *J. Non-Newtonian Fluid Mech.* **42**, 85–115.

Bird, R. B., Dai, G. C. & Yarusso, B. J. 1983 The rheology and flow of viscoplastic materials. *Rev. Chem. Engng* **1**, 1–70.

Burgess, S. L. & Wilson, S. D. R. 1996 Spin-coating of a viscoplastic material. *Phys. Fluids* **8**, 2291–2297.

Coussot, P. 1994 Steady, laminar, flow of concentrated mud suspensions in an open channel. *J. Hydr. Res.* **32**, 535–559.

Coussot, P. & Proust, S. 1996 Slow, unconfined spreading of a mudflow. *J. Geophys. Res.* **101**, 25217–25229.

Di Federico, V. 1998 Permanent waves in slow free-surface flow of a Herschel–Bulkley fluid. *Meccanica* **33**, 127–137.

Duffy, B. R. & Wilson, S. K. 1999 Thin-film and curtain flows on the outside of a rotating horizontal cylinder. *J. Fluid Mech.* **394**, 29–49.

Gans, R. F. 1999 On the flow of a yield strength fluid through a contraction. *J. Non-Newtonian Fluid Mech.* **81**, 183–195.

Huang, X. & Garcia, M. H. 1997 A perturbation solution for Bingham-plastic mudflows. *J. Hydraul. Engng ASCE* **123**, 986–994.

Huang, X. & Garcia, M. H. 1998 A Herschel–Bulkley model for mud flow down a slope. *J. Fluid Mech.* **374**, 305–333.

Lipscomb, G. G. & Denn, M. M. 1984 Flow of Bingham fluids in complex geometries. *J. Non-Newtonian Fluid Mech.* **14**, 337–346.

Liu, K. F. & Mei, C. C. 1989 Slow spreading of a sheet of Bingham fluid on an inclined plane. *J. Fluid Mech.* **207**, 505–529.

Liu, K. F. & Mei, C. C. 1990 Approximate equations for the slow spreading of a thin sheet of Bingham plastic fluid. *Phys. Fluids* A **2**, 30–36.

Liu, K. F. & Mei, C. C. 1994 Roll waves on a layer of a muddy fluid flowing down a gentle slope – a Bingham model. *Phys. Fluids* **6**, 2577–2590.

Moffatt, H. K. 1977 Behaviour of a viscous film on the outer surface of a rotating cylinder. *J. Méc.* **16**, 651–673.

Nusselt, W. 1916*a* Die Oberflächenkondensation des Wasserdampfes. *Z. Ver. Deutscher Ing.* **60**, 541–546.

Nusselt, W. 1916*b* Die Oberflächenkondensation des Wasserdampfes. *Z. Ver. Deutscher Ing.* **60**, 569–575.

O'Donovan, E. J. & Tanner, R. I. 1984 Numerical study of the Bingham squeeze film problem. *J. Non-Newtonian Fluid Mech.* **15**, 75–83.

Ross, A. B. 2000 Studies in non-Newtonian coating flows. PhD thesis, University of Strathclyde, Glasgow.

Tichy, J. A. 1991 Hydrodynamic lubrication theory for the Bingham plastic flow model. *J. Rheol.* **35**, 477–496.

Walton, I. C. & Bittleston, S. H. 1991 The axial flow of a Bingham plastic in a narrow eccentric annulus. *J. Fluid Mech.* **222**, 39–60.

Wilson, S. D. R. 1993 Squeezing flow of a Bingham material. *J. Non-Newtonian Fluid Mech.* **47**, 211–219.

Wilson, S. D. R. 1999 A note on thin-layer theory for Bingham plastics. *J. Non-Newtonian Fluid Mech.* **85**, 29–33.